



Hydrothermal Synthesis, Physical Characterization and Fluoride Adsorption of $\text{TiO}_2/\text{CeO}_2$

J. WU*, L. ZHOU, L. CHEN and J. ZHAO

College of the Environmental Science and Technology, Room No. 513, Minjing Building, Tongji University, Shanghai 200092, P.R. China

*Corresponding author: Fax: +86 21 65984261; Tel: +86 21 65984261; E-mail: wjj95-31952@163.com

(Received: 14 June 2011;

Accepted: 17 January 2012)

AJC-10967

Novel porous fluoride adsorbents were synthesized by co-doping CeO_2 and TiO_2 using hydrothermal method in the presence of the P123 ($\text{EO}_{20}\text{PO}_{70}\text{EO}_{20}$) as template. The physical properties of these resulting materials were characterized by X-ray diffraction, scanning electronic microscope and nitrogen adsorption/desorption isotherms and the results revealed that the materials had high surface area, uniformity in the ordered porous structure. The adsorption characteristics of fluoride on synthesized materials were studied using batch methods. The results showed that the adsorption isotherms on these adsorbents were correlated with the Langmuir and Freundlich adsorption equations and the adsorption capacity depended on contact time, initial fluoride concentration and adsorbents concentration, *etc.* The $\text{TiO}_2/\text{CeO}_2$ (1:1) exhibited the strongest adsorption capacity in all synthesized materials.

Key Words: Hydrothermal synthesis, Fluoride, Adsorption, $\text{TiO}_2/\text{CeO}_2$.

INTRODUCTION

All water on earth contains different level fluoride between trace level and several milligrams per litre. The major source of fluoride in water is considered to be fluorine-bearing minerals such as cryolite (Na_3AlF_6), fluor spar (CaF_2), apatite [$\text{Ca}_5(\text{PO}_4)_3\text{F}$]. More than 40 countries, including India^{1,2}, Mexico³, China, America and British⁴, face high concentration of fluoride in drinking water. The concentration of fluoride in water varies in relation to many factors—geological type, temperature, pH value, solubility of fluoride bearing minerals and complexed ions. Edmunds *et al.*⁵ gave a detail description for fluoride in nature waters. Besides the natural geological enrichment of fluoride in drinking waters, there can also be formidable contributions from industries. High-fluoride wastewaters can be generated by coal power plants, semiconductor manufacturing, glass and ceramic production, electroplating, rubber and fertilizer manufacturing. Fluoride concentration in industrial effluents is generally higher than that found in natural waters, ranging from tens to thousands of mg/L. A moderate amount of fluoride intake is confirmed to benefit to human health⁶, especially for the development tooth, dentin and bones for children⁷. As many studies shown, low doses of fluoride prevent from the development of bone and tooth, while high doses may lead to dental and skeletal fluorosis, changes of the skeleton, even other disorder such as parathyroid, kidney and live⁸, respectively. The most amount of fluoride in-taken

by human beings comes from drinking water, so World Health Organization (WHO) guideline for fluoride concentration in drinking water is 1.5 mg/L which complies with many UE standards. The maximum allowable concentration for fluoride in drinking water is 1 mg/L in China.

Various treatment technologies have been suggested for applying to remove fluoride from drinking waters. These methods can be divided into two groups: precipitation methods⁹ based on the addition of chemicals to the water and sorption methods¹⁰⁻¹⁵ in which the fluoride is removed by sorption or ion exchange reactions on some suitable substrate, capable of regeneration and reuse. Most methods for the fluoride removal suffer from one of the following drawbacks: high initial cost, lack of selectivity, low capacity and complicated or expensive regeneration. Sorption methods are more effective in reducing fluoride concentration than precipitation methods because of its merits such as high efficient, low cost and easy regeneration, *etc.* Except traditional adsorbent-activated alumina, in recent years, researches have paid more attention to many other adsorbents such as heat-treated soils, fly ash, silica gel, bone charcoal, spent catalyst and zeolites¹⁶⁻²¹. Microporous and mesoporous lanthanide oxide adsorbents have outstanding merits for removing fluoride ion from drinking water. Microporous and mesoporous materials have been identified as suitable matrices for many active rare earth ions or transition metal ions. Among microporous and mesoporous inorganic solids (with pore diameters of ≤ 2 and 2-50 nm, respectively)

have been found to behave as catalysts and adsorption media because of their large internal surface area. Mesoporous materials with unique properties such as high surface area, controlled pore structure and uniform pore size distribution are of great interest for adsorption, ions selection.

In this paper, we selected P123 (EO₂₀PO₇₀EO₂₀) as template, to synthesized porous adsorbent for fluoride ion by sol-gel and hydrothermal technologies. The adsorption process, structure and grain sizes were systematically examined.

EXPERIMENTAL

Pluronic P123 (EO₂₀PO₇₀EO₂₀), tetrabutyl titanate [Ti(OCH₂)₄] are all analytically grade. Cerium nitrates were prepared by dissolving CeO₂ in concentrated nitric acid. The synthesis of mesoporous TiO₂/CeO₂ was described in the following: 1 g of surfactant poly (ethylene glycol)-block-poly (propylene glycol)-block-poly (ethylene glycol) (P123) was first dissolved in 7.5 mL of deionized water and then 30 mL of dilute HCl solution (2.0 M) were added with stirring at 60 °C until a clear aqueous solution was obtained. Appropriate amounts of Ce(NO₃)₃ solution were added and mixed homogeneously. Then the 3.4 g of tetrabutyl titanate was added dropwise to the solution with stirring for 24 h and transferred into a teflon bottle sealed in an autoclave, which was heated at 100 °C for 24 h. The product was filtered, washed thoroughly with deionized water and dried at 75 °C. The as-synthesized material was calcined from room temperature to 550 °C at a heating rate of 2-6 °C/min for 5.5 h to remove the templates and obtained mesoporous materials.

Physical measurements: The particle size was characterized by means of X-ray diffraction (XRD, Bruke, D8-Advance, 40 kV and 20 mA, CuK_α). The morphology and microstructure were characterized with scanning electronic microscope (SEM, Philips XL-30). Nitrogen adsorption/desorption isotherms were measured at the liquid nitrogen temperature, using a Nova 1000 analyzer. Surface areas were calculated by the Brunauer-Emmett-Teller (BET) method and pore size distributions were evaluated from the desorption branches of the nitrogen isotherms using the Barrett-Joyner-Halenda (BJH) model.

Adsorption experiments: Adsorption experiments were carried out to determine the fluoride adsorption equilibrium and capacities of the TiO₂/CeO₂ adsorbents. Fluoride standard solutions with initial fluoride concentrations ranging from 1-30 mg/L were prepared by diluting a certain amount of a fluoride standard stock solution of 1000 mg/L with deionized water to a final volume of 100 mg/L. The pH of the standard solutions was adjusted to 7 with 0.10M NaOH and 5 % ammonia solution. For every experiment, 20 mL of the standard solution was mixed with about 0.10 g of the adsorbent material in a 50 mL high density polyethylene plastic bottle. The bottle was closed tightly and placed on an automatic shaker set at a shaking speed of 85 rpm for 2 h. After removing the bottles from the shaker, solution samples filtered and then 10 mL solution sample mixed with 10 mL of a total ionic strength adjustment buffer (TISAB III) and analyzed fluoride concentration. The fluoride concentration in water was determined electrochemically (Thermo, Orion 4-Star Plus pH/ISE Meter).

RESULTS AND DISCUSSION

The XRD patterns for these adsorbents were measured and showed the similar crystalline structure. Fig. 1 presented the selected XRD patterns of the TiO₂/CeO₂ (4:1) and TiO₂/CeO₂ (2:1) crystalline powders, respectively. The diffraction patterns for them were found to be exactly the same as that of TiO₂ reported in JCPDS Card. With adding to the amount of cerium ions, it presented some other crystal structure of CeO₂ and CeTi₂₁O₃₈. The crystal size was estimated from the broadening of the peaks by using the Scherrer formula:

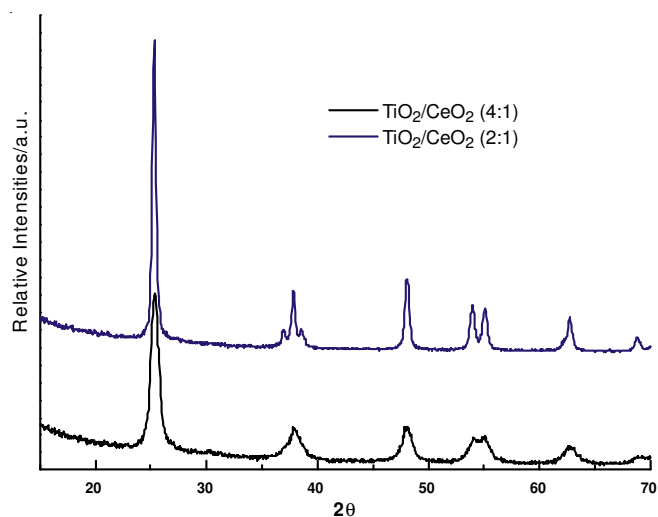
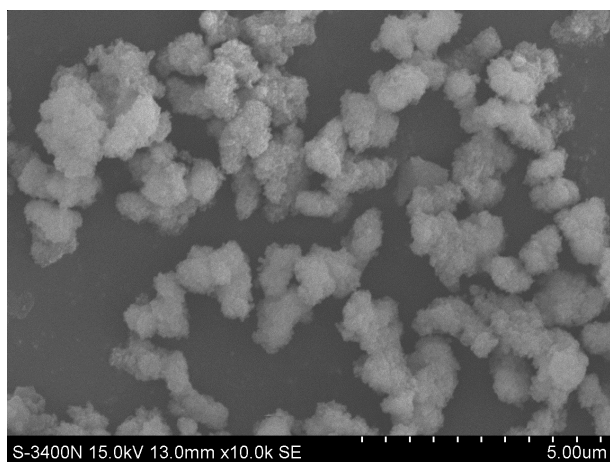


Fig. 1. XRD patterns of TiO₂/CeO₂ (4:1) and TiO₂/CeO₂ (2:1)

$$D_{hkl} = \frac{k\lambda}{[\beta(2\theta)\cos\theta]}$$

where $\beta(2\theta)$ is the width of the pure diffraction profile in radians, k is 0.89, λ is the wavelength of the X-rays (0.154056 nm), θ is the diffraction angle and D_{hkl} is the average diameter of the crystallite. By fitting various peaks to this formula and taking into account the instrumental broadening, it could be found that the particles was about 20 nm.

We further used the scanning electron microscope (SEM) to measure the TiO₂/CeO₂ (4:1) sample. Fig. 2 showed the representative SEM micrograph for TiO₂/CeO₂ (4:1). It could be seen that the product mainly consist of solid micron crystalline structures, which exhibit an interpenetrating network structures. The typical particle was estimated to be about 10 nm in dimension. It was clear that most of the particles present the spherical particles, mostly owing to the sol-gel treatment as reported²². In the sol-gel process, the o/w macro-emulsion is decisive and responsible for the final texture. The formation of isolated sphere is attributed to the weak interactions between the organic moieties such as van der Waals, London, or π - π stacking, which are able to induce an organization²³⁻²⁵. Besides this, the three-dimensional sizes of crystalline were very loose to afford high diffusion it need to refer these powders with high diffusion would be very useful for the application to obtain high efficient adsorbents because these microcrystalline materials can result in the huge surface area.

Fig. 2. SEM of TiO₂/CeO₂ (4:1)

N₂ adsorption-desorption isotherms were used as a macroscopic average measurement for exploring surface area, pore diameter and pore volume of the material. The N₂ adsorption-desorption isotherm of samples TiO₂/CeO₂ (4:1) and TiO₂/CeO₂ (2:1) were shown in Fig. 3. In accordance with the IUPAC classification²⁶, they both display type IV isotherms with H1-type hysteresis loops at relative pressure^{27,28}. As shown in Table-1, the specific area and the pore size were calculated by employing Brunauer-Emmett-Teller (BET) and Barrett-Joyner-Halenda (BJH) methods, respectively. After introducing Ce³⁺ ions, the adsorbents exhibited a small specific area and pore volume as increasing the amounts of doping Cerium ions. From the Table-1, the results showed that incorporation of cerium ions into TiO₂ resulted in the reduction of the surface area from 266.65 m²/g for the TiO₂/CeO₂ (4:1) to 76.13 m²/g for the TiO₂/CeO₂ (2:1), suggesting that micro-environment of mesopore template has moderately changed due to the introduction of different ions.

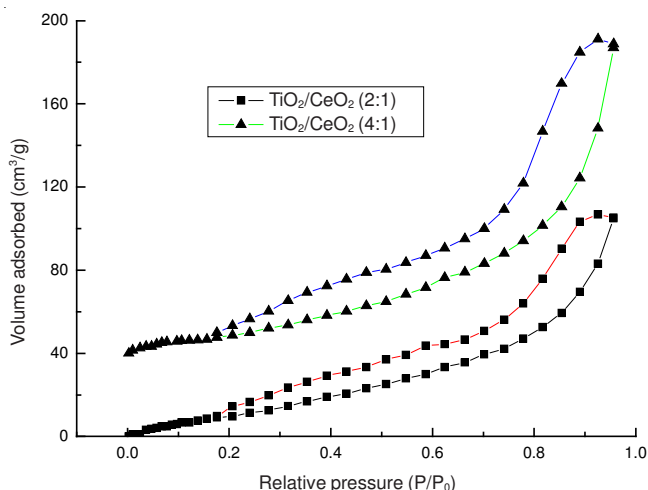
Fig. 3. N₂ adsorption/desorption isotherms of TiO₂/CeO₂ (4:1) and TiO₂/CeO₂ (2:1)

TABLE-1

TEXTURAL DATA OF TiO ₂ /CeO ₂ (4:1) AND TiO ₂ /CeO ₂ (2:1)			
Samples	S _{BET} (m ² /g)	V (cm ³ /g)	D _{BJH} (nm)
TiO ₂ /CeO ₂ (4:1)	266.65	0.207	6.650
TiO ₂ /CeO ₂ (2:1)	76.13	0.282	8.606

Fig. 4 showed the progression of adsorption reaction in different initial concentration of fluoride by TiO₂/CeO₂ after different contact times at a natural pH value of about 7²⁹. As contact time increased, fluoride removal also increased initially during the first contact time of 2 h, but then gradually approached a more or less constant value. As there was no increase in per cent fluoride removal between 2 and 6 h of contact time, an equilibrium time of 2 h was chosen and this was employed in all subsequent experiments. The rate of removal of fluoride was high in the initial 1 h, but thereafter the rate significantly levels off and eventually approaches zero, *i.e.*, equilibrium was attained. These changes might be due to the fact that, initially, all adsorbent sites were vacant and the solute concentration gradient was high. Afterwards, the fluoride uptake rate by the adsorbent decreases significantly, due to decrease in adsorption sites. A decreasing removal rate, particularly towards the end of the experiment, indicated a possible monolayer of fluoride ions on the outer surface and pores of adsorbent and pore diffusion onto the inner surface of adsorbent particles through the film due to continuous agitation maintained during the experiment.

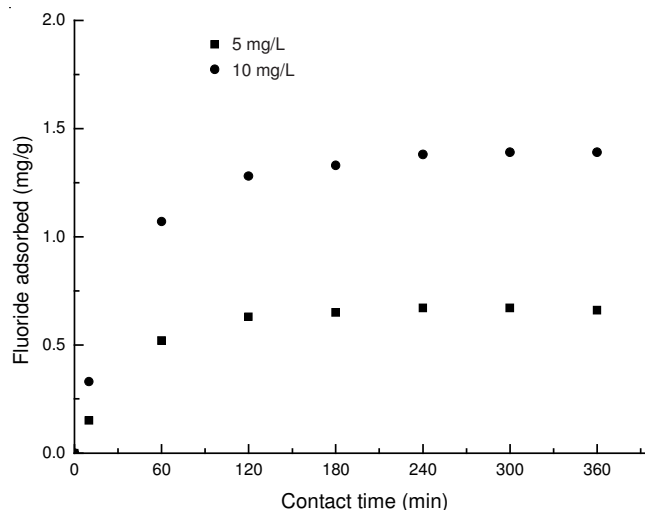


Fig. 4. Fluoride adsorption as a function of reaction time

Freundlich and Langmuir isotherm models were carried out to determine the fluoride adsorption equilibrium on TiO₂/CeO₂ in this work because these two models provide useful information for predicting the adsorption capacity of the adsorbent materials at given feed concentrations. The distribution of fluoride between the liquid phase and the solid phase is a measure of the position of equilibrium in the adsorption process and can be expressed by the Freundlich and Langmuir equations. These two models are widely used³⁰, the former being purely empirical and the latter assumes that maximum adsorption occurs when the surface is covered by the adsorbent. The Freundlich model is an indicative of surface heterogeneity of the sorbent and it is expressed as:

$$\log q_e = \log k + \frac{1}{n} \log c_e$$

where q_e (mg/g) is the amount of fluoride adsorbed per weight of adsorbent at equilibrium and c_e (mg/L) is the equilibrium concentration of the adsorbate in the solution, k is the

Freundlich constant representing the relative adsorption affinity of the adsorbent toward the adsorbate molecules and n represents the heterogeneity of the adsorbent. For the adsorbent in this work, the value of k was 0.67 mg/g and $1/n$ was 0.52.

The Langmuir equation, which is valid for monolayer sorption onto a surface with a finite number of identical sites, is given by the following equation:

$$\frac{1}{q_e} = \frac{1}{q_0 b} \times \frac{1}{c_e} + \frac{1}{q_0}$$

where q_0 (mg/g) represents the monolayer adsorption capacity, b (L/mg) is the Langmuir constant that characterizes the adsorbent-adsorbate interaction. The linear plot of $1/q_e$ versus $1/c_e$ (Fig. 5) indicated the applicability of Langmuir adsorption isotherm. The values of Langmuir parameters, q_0 and b were 0.27 mg/g and 0.47 L/mg, respectively.

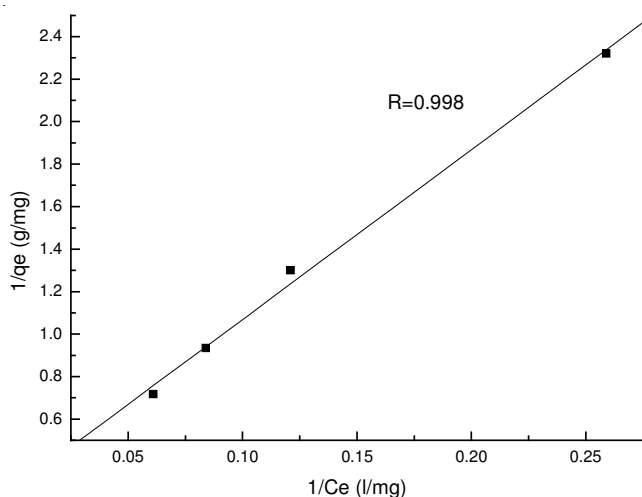


Fig. 5. Langmuir plot for the adsorption of fluoride

The capacity of fluoride removal by $\text{TiO}_2/\text{CeO}_2$ depended on the doping concentration of cerium ions. The concentration increase of the Ce^{3+} ions, however, the adsorbent capacity was saturated and begins to decrease at over a critical maximum volume. That is to say, if the ratios excess certain value, phenomenon of adsorption capacity decreased occurred. As shown in Table-2, it was obvious that the intensity of the adsorption had constantly increased with the increase the concentration of Ce^{3+} at the ratio of Ce to Ti being the range from 0.2 to 1.0. When Ce:Ti > 1, the fluoride removal decreased.

TABLE-2 ADSORPTION VOLUME ON ADSORBENTS SYNTHESIZED WITH DIFFERENT RATIO OF Ti to Ce				
Samples	$\text{TiO}_2/\text{CeO}_2$ (4:1)	$\text{TiO}_2/\text{CeO}_2$ (2:1)	$\text{TiO}_2/\text{CeO}_2$ (1:1)	$\text{TiO}_2/\text{CeO}_2$ (2:3)
Adsorption	0.41 mg/g	0.43 mg/g	0.53 mg/g	0.46 mg/g

Conclusion

In summary, fluoride removal adsorbents $\text{TiO}_2/\text{CeO}_2$ were synthesized by sol-gel technology and hydrothermal methods

at 100 °C. All physical measurements such XRD, SEM and N_2 adsorption-desorption isotherms results indicated that these adsorbents exhibited a novel crystalline with micrometer dimension. The $\text{TiO}_2/\text{CeO}_2$ is a suitable adsorbent for the removal of fluoride from water. The removal of fluoride from aqueous solutions strongly depended on the contact time, the ratio of Ti to Ce and adsorbent concentration. The adsorption process fitted the Langmuir and Freundlich isotherms and $\text{TiO}_2/\text{CeO}_2$ (1:1) presented the strongest adsorbate intensity in all synthesis samples.

ACKNOWLEDGEMENTS

The work was supported by National Science & Technology Pillar Program in the Eleventh Five-year Plan Period of China (2006BAJ04A07).

REFERENCES

1. Meenakshi, V.K Garg, Kavita, Renuka and A. Malik, *J. Hazard. Mater.*, **106**, 85 (2004).
2. A.K. Misra and A. Mishra, *J. Hazard. Mater.*, **144**, 438 (2007).
3. M. Grimaldo, V.H. Borjaaburto, A.L. Ramirez, M. Ponce, M. Rosas and F. Diazbarriga, *Environ. Res.*, **68**, 25 (1995).
4. C. Neal, M. Neal, H. Davies and J. Smith, *Sci. Total Environ.*, **314-316**, 209 (2003).
5. W.M. Edmunds and P.L. Smedley, In ed.: O. Selenus, Fluoride in Natural Waters-Occurrence, Controls and Health Aspects. Medical Geology Reference-Earth Science Information in Support of Public Health Protection, Academic, pp. 301-329 (2005).
6. M.K. Malde, A. Maage, E. Macha, K. Julshamn and K. Bjorvatn, *J. Food Compos. Anal.*, **10**, 233 (1997).
7. D.C. Clark, *Can. Med. Assoc. J.*, **149**, 1787 (1993).
8. X.Z Xiong, J.L. Liu, W.H. He, T. Xia, P. He, X.M. Chen, K.D. Yang and A.G. Wand, *Environ. Res.*, **103**, 112 (2007).
9. N. Mameri, A.R. Yeddou, H. Lounici, D. Belhocine, H. Grib and B. Bariou, *Water Res.*, **32**, 1604 (1998).
10. K.M. Popat, P.S. Anand and B.D. Dasare, *React. Polym.*, **23**, 23 (1994).
11. N. Kabay and H. Kodama, *Solv. Extr. Ion Exch.*, **18**, 583 (2000).
12. H. Kodama and N. Kabay, *Solid State Ionics*, **141-142**, 603 (2001).
13. C.L. Yang and R. Dluhy, *J. Hazard. Mater.*, **94**, 239 (2002).
14. S. Ghorai and K.K. Pant, *Chem. Eng. J.*, **98**, 165 (2003).
15. Y. Zhou, C. Yu and Y. Shan, *Purif. Technol.*, **36**, 89 (2004).
16. A.K. Chaturverdi, K.P. Yadava, K.C. Pathak and V.N. Singh, *Water Air Soil Pollut.*, **49**, 51 (1990).
17. R. Wang, H. Li, P. Na and Y. Wang, *Water Qual. Res. J. Can.*, **30**, 81 (1995).
18. S.A. Wasay, M.J. Haron and S. Tokunaga, *Water Environ. Res.*, **68**, 295 (1996).
19. D.S. Bhargava and D.J. Killedar, *Water Res.*, **26**, 781 (1992).
20. Y.D. Lai and J.C. Liu, *Separat. Sci. Technol.*, **31**, 2791 (1996).
21. S. Mayadevi, *Ind. Chem. Eng.*, **38**, 155 (1996).
22. B. Yan, L. Zhou and Y. Li, *Colloid Surf. A: Physicochem. Eng. Aspects.*, **350**, 147 (2009).
23. H.F. Lu and B. Yan, *J. Photochem. Photobiol. A: Chem.*, **194**, 136 (2008).
24. B. Boury, F. Ben, R.J. Corriu, P. Delord and M. Nobili, *Chem. Mater.*, **14**, 730 (2002).
25. B. Boury and R.J. Corriu, *Chem. Commun.*, **21**, 795 (2002).
26. A. Laachir, V. Perichon, A. Badri, J. Lamotte, E. Catherine, J.C. Lavalley, J.E. Fallah, L. Hilarer, F.L. Normand, E. Uenere, G.N. Sauvion and O. Touret, *J. Chem. Soc. Faraday Trans.*, **87**, 1601 (1991).
27. M.C. Goncalves, V.D. Bermudez, R.A. Sa Ferreira, L.D. Carlos, D. Ostrovskii and J. Rocha, *Chem. Mater.*, **16**, 2530 (2004).
28. M. Ignatovych, V. Holovey, A. Watterich, T. Vidoczy, P. Baranyai, A. Kelemen and O. Chuiko, *Radiat. Meas.*, **38**, 567 (2004).
29. S. Ghorai and K.K. Pant, *Sep. Purif. Technol.*, **42**, 265 (2005).
30. L.M. Camacho and A. Torres, *J. Colloid. Interf. Sci.*, **349**, 307 (2010).